# Composite trait Mendelian Randomization reveals distinct metabolic and lifestyle consequences of differences in body shape

Jonathan Sulc[1,2], Anthony Sonrel[2,3], Ninon Mounier[1,2], Chiara Auwerx[1,2,4], Eirini Marouli[5,6], Liza Darrous[1,2], Bogdan Draganski[7,8], Tuomas O. Kilpeläinen[9], Peter Joshi[10], Ruth J.F. Loos[11,12,13], Zoltán Kutalik*[1,2,14]

[1] University Center for Primary Care and Public Health, University of Lausanne, Switzerland

[2] Swiss Institute of Bioinformatics, Lausanne, Switzerland

[3] Department of Molecular Life Sciences, University of Zürich, Switzerland

[4] Center for Integrative Genomics, University of Lausanne, Switzerland

[5] William Harvey Research Institute, Barts and The London School of Medicine and Dentistry, London, United Kingdom of Great Britain and Northern Ireland

[6] Centre for Genomic Health, Life Sciences, London, United Kingdom of Great Britain and Northern Ireland

[7] Laboratory for Research in Neuroimaging, Department of Clinical Neurosciences, Lausanne University Hospital and University of Lausanne, Lausanne, Switzerland

[8] Neurology Department, Max-Planck Institute for Human Cognitive and Brain Sciences, Leipzig, Germany

[9] Novo Nordisk Foundation Center for Basic Metabolic Research, Faculty of Health and Medical Sciences, University of Copenhagen, Copenhagen, Denmark

[10] Centre for Global Health Research, Usher Institute, University of Edinburgh, Edinburgh, UK.

[11] The Charles Bronfman Institute for Personalized Medicine, Icahn School of Medicine at Mount Sinai, New York, New York, United States of America.

[12] The Mindich Child Health and Development Institute, Icahn School of Medicine at Mount Sinai, New York, New York, United States of America.

[13] Department of Environmental Medicine and Public Health, Icahn School of Medicine at Mount Sinai, New York, New York, United States of America.

[14] Genetics of Complex Traits, University of Exeter Medical School, University of Exeter, Exeter, UK

* Corresponding author

**Abstract**

Obesity is a major risk factor for a wide range of cardiometabolic diseases. As its genetic determinants have become increasingly elucidated, it has become feasible to investigate its health consequences via Mendelian randomisation (MR). To study the impact of different aspects of body morphology on health outcomes, we gathered fourteen body morphology measures and associated GWAS summary statistics from UK Biobank and used principal component analysis to reveal four major independent axes of genetically driven variation in body shape and size: overall body size, adiposity, predisposition to abdominal fat deposition, and lean mass. Enrichment analyses suggest that body size and adiposity are affected by genes involved in neuronal signalling, whereas body fat distribution and lean mass are dependent on genes involved in morphogenesis and energy homeostasis. Using MR, we found that the adiposity component had the strongest impact on cardiometabolic health and obesity-related diseases and its genetic basis was intertwined with aspects of lower socio-economic status (SES). Overall body size affected many of the same diseases in an independent manner, but was linked to a more sedentary lifestyle with no change in SES. The body mass-neutral component predisposing to abdominal fat deposition, likely reflecting a shift from subcutaneous to visceral fat, exhibited health effects that were weaker but more specifically linked to lipotoxicity, such as diabetes and heart disease. The presented decomposition approach sheds light on the biological mechanisms underlying the remarkably heterogeneous nature of body morphology as well as its consequences on health and lifestyle.

# Introduction

Obesity is one of the main risk factors for many non-communicable diseases, such as type 2 diabetes (T2D, reviewed in 1) and cardiovascular diseases (CVD, reviewed in 2). The associated disease risk and underlying biology of obesity are generally studied through the lens of body mass index (BMI, weight [kg] / height$^2$ [m$^2$]), which uses excess body mass as a surrogate for adiposity. This approximation provides a reasonably accurate predictor at the population level[3,4] but is blind to many aspects of body shape and composition that may be critical to disease etiology. Indeed, disease risk and progression have been shown to be affected by the location and type of the adipose tissue in which excess calories are stored[3–6]. Abdominal obesity in particular, usually assessed using waist circumference or waist-to-hip ratio (WHR), is associated with increased disease risk and mortality independent of BMI[3].

Although the exact mechanisms underlying the consequences of adiposity on health have not been fully elucidated, the predominant hypothesis is that of adipose tissue expandability: that excess calories are preferentially stored in subcutaneous adipose tissue (SAT), which can expand with little to no deleterious impact on health[7,8]. When its capacity for expansion is exceeded, adipose cells hypertrophy, causing local inflammation, and fat is increasingly stored as ectopic fat in organs and as visceral adipose tissue (VAT) around organs in a process similar to a mild form of lipodystrophy. Ectopic and visceral fat are thought to play a central role in many of the direct consequences of obesity.

Much remains unknown about the genetic and environmental factors affecting body fat distribution and its contribution to health outcomes. Currently available non-invasive imaging techniques such as magnetic resonance imaging (MRI) and dual-energy X-ray absorptiometry (DXA) allow the accurate measurement of adipose mass in different parts of the body and have significantly contributed to our understanding of the impact of different subtypes of adiposity on

health[9,10]. Such techniques remain costly and are therefore generally restricted to smaller sample sizes.

An alternative approach is the concurrent analysis of multiple traits, leveraging the concurrent changes in multiple phenotypes to understand the underlying causes and mechanisms. Analysis of variance methods, such as principal component analysis (PCA), have been used to investigate the complex architecture underlying body morphology, revealing the main axes of phenotypic variation and increasing the statistical power to detect novel loci affecting body morphology[11]. While this has improved our understanding of the genetic basis underlying common and distinct components of anthropometric traits, their impact on health and quality of life remains unknown. Other approaches such as clustering and canonical correlation analysis (CCA) have identified single nucleotide polymorphisms (SNPs) associated with healthier metabolic profiles, despite higher BMI and/or body fat percentage[12–15]. However, these hypothesis-driven approaches (i.e. identifying clusters of functionally similar SNPs based on both obesity measures and health outcomes) are not suited to determine the causality of these correlated differences or the directionality of potential causal effects because the SNP groups by construction have different health consequences.

Here we followed a hypothesis-free approach to isolate independent axes of variations in body shape and size and investigated their health consequences. We performed a PCA on GWAS summary statistics of 14 anthropometric traits from the UK Biobank[16] to extract orthogonal components, each representing different features of body shape (Figure 1). We show that these measures of body shape can be summarized using four principal components (PCs) affecting body size, adiposity, abdominal fat deposition, and lean mass, respectively. Enrichment analyses highlighted differences in the pathways and tissues involved in these composite traits, providing new insight into the underlying biological mechanisms. We then used robust cross-sex Mendelian randomization to assess the impact of these independent components on health and lifestyle. While many health and lifestyle consequences were shared

with individual traits, these orthogonal PCs allowed us to better disentangle the independent contributions of different aspects of body shape. The results can be explored using the shiny app which can be downloaded by following the instructions at http://wp.unil.ch/sgg/pca-mr/.

# Results

## PCA of effect sizes

A schematic representation of our composite MR analysis framework is shown in Figure 1. We selected 14 anthropometric and bioimpedance-derived traits available in the UK Biobank[16] as the basis for the principal component analysis (PCA). The genome-wide summary statistics for these were made available by the Neale lab (www.nealelab.is/uk-biobank), in addition to which we included waist-to-hip ratio (WHR) with summary statistics from a meta-analysis of data from both the UK Biobank and the GIANT consortium[17], all of which were available in three sex groups: men, women, and both sexes combined. Genome-wide significant (GWS) SNPs (p-value $< 5*10^{-8}$ for any trait) were pruned for independence. The resulting SNP x traits matrix of effect estimates was subjected to PCA. The loadings of each principal component (PC) were then rescaled according to the phenotypic correlation between these traits in the UK Biobank so as to obtain standardised effect sizes, i.e. the resulting PC phenotypes would have a variance of 1. This analysis was performed using men-only, women-only, and sex-combined samples.

The top four PCs explained more than 99% of the total variance and had similar loadings in all three sex groups. PC1 (women: 72.4% variance explained; men: 78.6%; combined: 72.4%) represents an overall increase in body size, with positive weights for all traits indicating a slightly disproportionate increase in body mass, both fat and lean, compared to height, resulting in higher BMI as well (Figure 2, Supplementary Tables 3–5). PC2 (women: 17.9%; men: 17.3%; combined: 20.3%) shows a decrease in height but an increase in fat mass at the expense of

lean mass (Figure 2, Supplementary Tables 3–5). PC3 (women: 6.3%; men: 1.1%; combined: 4.2%) is BMI- and body fat mass-neutral, decreasing hip circumference, and increasing waist circumference and WHR, reflecting a shift in body fat from hips to waist (Figure 2, Supplementary Tables 3–5). PC4 (women: 2.9%; men: 2.5%; combined: 2.5%) resulted in decreased height and increased BMI, with an increase in lean mass at the expense of fat mass (Figure 2, Supplementary Tables 3–5).

PC loadings were highly concordant between sex groups and produced highly correlated associations between SNPS and composite traits for all PCs (all $r > 0.81$, see Supplementary Figure 1), although the relative importance of PC3 (predisposition to abdominal fat deposition) and PC4 (lean mass) were switched in men due to lower explained variance of PC3 in men compared to women (1.1% in men vs. 6.3% in women). For clarity, we use the numbering common to women and combined sexes, e.g. “PC3” refers to the body mass-neutral component predisposing to abdominal fat deposition in all sex groups (despite being fourth in terms of explained variance in men). Despite a considerable change in explained variance, the SNP effect estimates for PC3 were highly correlated across all sex groups (all pairwise $r > 0.96$). The high correlation of effect estimates for each PC between sex groups suggests that the underlying biological mechanisms are the same.

In fact, PCs derived from men-specific data were generally more similar to those from women-specific data than either were to PCs from combined-sex data (Supplementary Figure 1), with the exception of abdominal fat distribution (PC3), which is related to the highly sex-specific WHR. We therefore decided to use sex-specific PCA loadings rather than those from sex-combined data. We chose to use women-specific loadings for all groups, as a single set of loadings (rather than using the loadings from whichever sex is used as exposure) ensured the equivalence of the resulting composite trait. The selection of women- over men-specific loadings was driven by larger amounts of variance explained by lower PCs, which increased our statistical power to detect causal effects. These women-specific loadings were then applied to

sex-specific genetic effect estimates to obtain the sex-specific SNP effects for each PC. Using those from men produced similar results but reduced the power for PC3 in particular.

We found 1064 independent GWS SNPs associated with PC1 (body size), 593 with PC2 (adiposity), 464 with PC3 (predisposition to abdominal fat deposition), and 203 with PC4 (lean mass). Among these, 5.2 - 7.5% were not GWS for any individual trait, representing 65, 31, 35, and 14 additional SNPs, respectively.

Note that PCs obtained were robust to changes in the selection of specific traits, mainly resulting in changes in the explained variance (potentially reordering them). For example, excluding both height and WHR reduced the statistical power and provided fewer instruments, but yielded effect estimates which were highly correlated with those obtained using the full set of traits (all $r > 0.88$, $p < 10^{-95}$, see Supplementary Figure 2).

## Tissue/pathway enrichment

We tested the PCs for enrichment of genes expressed in specific tissues using the MAGMA method[18] through the FUMA interface[19] in both GTEx v8[20] and brain development and aging data from BrainSpan[21]. We also tested for their enrichment of molecular pathway terms from the DEPICT dataset[22] using PASCAL[23].

The tissue-enrichment results of the four PCs as well as weight, BMI and WHR are shown in Figure 3 and listed in Supplementary Tables 6–9. Loci associated with PC1 (body size) were enriched for genes expressed in the cerebellum ($p < 10^{-4}$) and the pituitary gland ($p < 10^{-5}$). Weight showed similar enrichment, in addition to the frontal cortex of the brain which did not pass multiple testing correction for PC1.

While loci associated with PC2 (adiposity) were also somewhat enriched for genes expressed in the pituitary ($p = 1.8*10^{-3}$), it was most highly enriched for those expressed in cerebellum ($p < 10^{-11}$) and other parts of the cerebral cortex (frontal cortex, and anterior cingulate, all $p < 1.6*10^{-3}$). Using data from BrainSpan[21], we found adiposity (PC2) to be

enriched for genes expressed in the brain specifically during the early to late mid-prenatal phase of development ($p < 10^{-3}$). BMI was similarly enriched with a slight trend for stronger enrichment, leading to additional areas of the brain becoming significant (basal ganglia, hippocampus, hypothalamus, and amygdala).

PC3 (predisposition to abdominal fat deposition) was most strongly enriched for genes expressed in SAT ($p = 10^{-18}$), followed by VAT ($p = 4*10^{-13}$), female reproductive tissues (breast mammary tissue, ecto- and endocervix, and uterus, all $p < 6*10^{-14}$), and nerves (tibial, $p = 2*10^{-15}$). Other significantly enriched tissues are shown in Figure 3 and listed in Supplementary Tables 6–9. Note that using male-specific summary statistics and PC loadings with the same gene expression datasets produced a similar enrichment for female-specific tissues. WHR was only enriched for a fraction of these tissues and much weaker. Both PC3 and WHR were also enriched for genes expressed in the prenatal brain.

Similarly, PC4 (lean mass) was strongly enriched for genes expressed in female-specific tissues (uterus, ecto- and endocervix, all $p < 10^{-9}$), arteries ($p < 3*10^{-7}$), oesophagus muscularis and gastroesophageal junction ($p < 10^{-7}$), as well as the prenatal brain ($p < 1.6*10^{-3}$). Other significant tissues are shown in Figure 3 and listed in Supplementary Tables 6–9.

The analysis of molecular pathways showed qualitatively similar enrichment for PCs 1 and 2, weight and BMI (Figure 4, Supplementary Table 10). These were mostly terms related to the brain, synapses, behaviour, or learning.

PC3 had the most numerous enriched terms and the strongest enrichment overall. Most of the enriched terms were not related to brain function, but to embryogenesis and morphology, with many others specifically concerning adiposity, metabolism, and glucose homeostasis (Figure 4, Supplementary Table 10). Other terms were related to vascular or heart function, or hormones. Enrichment for WHR was somewhat similar to both BMI and PC2 but weaker than either for almost all terms.

PC4 showed some overlap in terms with PC3, mainly in terms related to embryogenesis and morphology (Figure 4, Supplementary Table 10).

## Mendelian Randomization analysis

### Cross-sex MR to avoid bias from sample-overlap

We used inverse-variance weighted (IVW) Mendelian randomisation (MR) to test for causal effects of the 14 anthropometric traits and PCs on disease outcomes, continuous measures of health, lifestyle factors, diet, and brain imaging-derived phenotypes (IDPs), as well as the reverse. To avoid bias in the MR estimates due to sample overlap, we used sex-specific effects from opposite sexes for exposures and outcomes (male exposure - female outcome and female exposure - male outcome, always using female loadings for PCs). This should produce unbiased estimates of the causal effects in the sex used in the outcome, provided the strength of the instruments' association with the exposure was not different between sexes. The two sex-specific causal effect estimates were meta-analysed using inverse-variance weighting. Where the strength of the instruments' association with the exposure differed between sexes, namely for WHR and PC3 (abdominal fat distribution), the causal effect estimates may be biased (generally towards the null). Although the effect size estimates may be slightly over- or underestimated, this should not affect the type I error rate (see Methods). Sex-specific causal effect estimates were obtained using the summary statistics for the sex of interest in the outcome and the opposite for exposure, provided that the genetic effects in the exposure were similar between sexes.

The meta-analysed estimate was on average 35% lower than those derived directly from estimates from the same sample (see Supplementary Figures 3–30). This reduction was largest for traits related to lean mass such as leg lean mass (47%) and weaker for fat mass-related

traits such as trunk fat mass (15%). The magnitude of this decrease was similar for PCs, ranging from 28% to 45%, with the strongest decrease seen in PC1 (body size).

To assess the validity of these meta-analysed causal estimates, we applied this approach to effect estimates for BMI from GIANT[24] as exposure with those from the UK Biobank as outcome. As these were calculated in independent cohorts, the casual effects estimated using cross-sex MR and IVW MR should be the same. The causal effect estimates obtained from both methods were highly correlated (all $r \geq 0.92$, $p < 1.9*10^{-8}$, see Supplementary Figures 31–34). We found none of the individual effect estimates to be significantly different between the two approaches, although there was a nominally significant tendency for causal effects from the cross-sex MR to be slightly lower for disease risk (TLS slope = 0.96, $p = 0.034$) and lifestyle (TLS slope = 0.91, $p = 0.022$).

With these same exposure effect estimates, we were also able to test whether using effect estimates for the sex of interest for the outcome but the opposite sex for exposure provided a suitable approximation of sex-specific causal effects. The causal effect estimates were highly consistent between the two approaches (r between 0.84 and 0.93, $p < 1.8*10^{-10}$) and none of the individual estimates was significantly different (Supplementary Figures 35–42). Only the male-specific effects on diet tended to be underestimated when using female-specific effect estimates for BMI as exposure (TLS slope = 0.83, $p = 0.0054$).

The use of weighted median MR rather than IVW produced similar results. The correlation between causal effect estimates was generally above 0.95 (see Supplementary Figures 43–70), though somewhat weaker for exposures with fewer instruments, such as PC4 where the correlation coefficient was 0.8. The estimated strength of causal effects was highly consistent as well (TLS slope between 0.85 and 1), though generally slightly lower for median-based MR. Despite similar estimates, the decreased power of median-based MR also resulted in fewer effects being significant.

## Individual vs. composite phenotypes

For simplicity, we will mainly describe the individual phenotypes which are most useful for comparison with the obtained PCs, namely weight, BMI, and WHR. These are the most commonly used measures of obesity and each of these was highly correlated with one of the top three PCs ($r \geq 0.80$, see Supplementary Figure 71 and Supplementary Table 11). Other phenotypes were somewhat correlated to these traits (Supplementary Table 11) and had similar or weaker consequences on the selected outcomes (e.g. the effects of body fat percentage and BMI on disease had a correlation coefficient $r = 0.95$, $p = 2.3*10^{-43}$, see Supplementary Tables 12–15 for the full results).

For the purpose of comparing phenotypes, whether individual or composite, in terms of their consequences, we used the coefficients and corresponding p-values for the Pearson correlation of their effects. Where the effects were strongly correlated, we used TLS regression to compare the ratio of effects between exposures. The comparisons were made using the effects on disease risk as this category presented the largest number of outcomes, leading to greater statistical power and decreased variance. The results were similar for other categories.

The effects of weight and WHR were quite strongly correlated with those of BMI (r between 0.84 and 0.87), though BMI tended to have stronger effects than either (TLS slope between 1.55 and 1.61, $p_{slope \neq 1} < 5.1*10^{-12}$). The effects of weight and WHR were slightly less correlated ($r = 0.59$).

The effects of PC1 (body size), PC2 (adiposity), and PC3 (abdominal fat deposition) on diseases were strongly correlated with those of weight, BMI, and WHR, respectively ($r_{PC1\text{-}weight} = 0.95$, $r_{PC2\text{-}BMI} = 0.97$, $r_{PC3\text{-}WHR} = 0.88$). Despite this similarity between PCs and traits, the phenotypic correlation between PCs was much lower than was the correlation between individual phenotypes (e.g. the phenotypic correlation between PC1 and PC2 was only 0.33 while it was 0.84 between BMI and weight, Supplementary Figure 72, Supplementary Table 11),

which resulted in lower correlation between their effects as well (e.g. correlation between PC1 and PC2 effects on diseases was 0.56 *vs* 0.84 between BMI and weight). These observations confirm that although PCs 1-3 bear similarity with their single trait counterparts (weight, BMI, WHR), they represent a more orthogonal dissection of the underlying anthropometric phenomena. Note that the phenotypic realisation of PCs are not orthogonal, and their correlation is therefore not zero (Supplementary Table 11), due to correlation in environmental factors affecting them. This does not affect the independence of the MR causal effect estimates.

The effects of PC4 (lean mass) were fewer than for other PCs and only nominally negatively correlated with those of standing height (r = -0.27).

## Disease risk

PC1 (body size) and weight both increased the risk of many diseases (Figure 5, Supplementary Table 12). An increase of 1 standard deviation in these exposures (corresponding to a 14.3 and 13.9 kg increase in weight in men and women, respectively) increased the absolute risk of diabetes by 1.4% for PC1 and 2.2% for weight, that of arthrosis by 2.0 and 2.6%, respectively, as well as many other diseases such as nerve disorders, diseases of the veins and circulatory system, and prolapsed disc. Although both increased the risk of cardiac arrhythmias by nearly 1%, they did not significantly affect the risk of hypercholesterolemia or heart disease. The largest difference between the effects of these exposures was for hypertension, which was among the strongest for weight ($b = 0.092$, $p = 2.1*10^{-16}$) but much weaker and only nominally significant for PC1 ($b = 0.036$, $p = 1.8*10^{-4}$, $p_{diff} = 1.7*10^{-4}$).

PC2 (adiposity) and BMI both had much stronger effects on many obesity-related diseases (Figure 5, Supplementary Table 12), where a 1 SD increase in these exposures (corresponding to a 4.2 and 5.1 kg/m$^2$ increase in BMI for men and women, respectively) led to a 3.6 and 3.9% increased risk of diabetes ($p < 2.7*10^{-59}$) and that risk of hypertension by as much as 10.3 and

9.8% ($p < 2.0*10^{-71}$), respectively. They also increased the risk of hypercholesterolemia by more than 3% and ischaemic heart disease by 2.1 and 1.8%, respectively. The risk of many other diseases such as arthrosis and diseases of the nervous system were also increased.

PC3 (predisposition to abdominal fat deposition), despite being weight- and BMI-neutral, was a risk factor for many of the same obesity-related diseases as PC2 and BMI (Figure 5, Supplementary Table 12). A 1 SD increase in PC3 increased the risk of diabetes by 1.8% ($b = 0.094$, $p = 8.7*10^{-22}$), hypertension by 5.0% ($b = 0.11$, $p = 1.7*10^{-26}$), hypercholesterolemia by 3.2% ($b = 0.098$, $p = 2.5*10^{-24}$), and ischaemic heart disease by 1.5% ($b = 0.063$, $p = 9.2*10^{-13}$). Although these effects were correlated with those of WHR, they tended to be slightly weaker (TLS slope = 1.62, $p = 2.7*10^{-23}$) due to WHR including effects attributable to the accumulation of excess fat mass (similar to BMI and PC2). WHR also increased the risk of joint diseases, such as arthrosis ($b = 0.06$, $p < 2.5*10^{-5}$).

Lean mass (PC4) had few consequences on health, only significantly increasing the risk of nerve disorders by 1.1% ($b = 0.063$, $p = 1.4*10^{-8}$) and carpal tunnel syndrome by 1% ($b = 0.071$, $p = 5.7*10^{-9}$).

### Continuous health outcomes

The changes in continuous measures of health and body function were overall consistent with those observed in disease outcomes (Supplementary Table 13).

PC1 and weight both increased diastolic, but not systolic, blood pressure (DBP, $b > 0.053$, $p < 3.4*10^{-7}$) and decreased the maximum heart rate during fitness test ($b < -0.16$, $p < 3.5*10^{-17}$). Creatinine (enzymatic) and potassium in urine, two indicators of kidney function, were both increased (b between 0.084 and 0.13, $p < 2.4*10^{-22}$). PC1 (body size) but not weight was strongly associated with increased forced vital capacity (FVC, $b = 0.21$, $p = 2.6*10^{-51}$, $p_{diff} = 3.4*10^{-22}$), which can be explained by height being an important component of PC1.

PC2 and BMI increased both systolic and diastolic BP ($b_{all} > 0.13$, $p_{all} < 2.6*10^{-23}$), as well as pulse rate (PC2: b = 0.081, p = $6.8*10^{-8}$; BMI: b = 0.075, p = $10^{-7}$). Both decreased FVC (p < $1.1*10^{-28}$), but the effect was significantly greater for PC2 (adiposity) (PC2: b = -0.28; BMI b = -0.14; $p_{diff} = 4.5*10^{-13}$). BMI also decreased maximum heart rate during fitness test (b = -0.14, p = $1.2*10^{-8}$). Both PC2 and BMI increased creatinine (enzymatic) and sodium in urine (b = [0.078 – 0.13], p < $7.4*10^{-10}$).

PC3 and WHR increased systolic BP (PC3: b = 0.064, p = $1.3*10^{-9}$; WHR b = 0.095, p = $3.8*10^{-13}$), but only WHR significantly increased diastolic BP (b = 0.083, p = $1.1*10^{-9}$). Both also decreased FVC (p < $5.9*10^{-5}$), though the effect was three times greater for WHR (PC3: b = -0.049; WHR: b = -0.15; $p_{diff} = 8.9*10^{-8}$).

PC4 had no significant effects on continuous health measures.

None of these exposures had significant effects on the molecular phenotypes in blood such as cholesterol or glucose levels.

### Lifestyle factors

PC1 (body size) and weight increased smoking and exposure to tobacco smoke as well as overall alcohol consumption, particularly spirits (Figure 6, Supplementary Table 14). These changes are consistent with reduced SES, as exemplified by an increased TDI (weight: b = 0.045, p = $2.9*10^{-7}$; nominally significant for PC1: b = 0.023, p = $2.2*10^{-3}$) and a longer working week (weight: b = 0.057, p = $1.3*10^{-8}$; PC1: b = 0.051, p = $2.4*10^{-8}$). This was also accompanied with a reduction of physical activity, such as less frequent stair climbing and reduced walking pace.

Both PC2 (adiposity) and BMI were associated with a strong reduction in socio-economic status (SES) (Figure 6, Supplementary Table 14), as shown by increased TDI (PC2: b = 0.098, p = $4.9*10^{-19}$; BMI: b = 0.077, p = $1.1*10^{-13}$), greater probability of a job involving heavy physical work (PC2: b = 0.13, p = $4.1*10^{-17}$; BMI: b = 0.091, p = $4.5*10^{-9}$), as well as reduced income

(PC2: b = -0.15, p = $7.3*10^{-36}$; BMI: b = -0.12, p = $7.3*10^{-22}$) and education (PC2: b = -0.19, p = $1.4*10^{-39}$; BMI: b = -0.14, p = $5*10^{-20}$). PC2, but not BMI, was also associated with lower fluid intelligence score (b = -0.2, p = $6.8*10^{-19}$, $p_{diff} = 3*10^{-5}$). Accompanying these were other changes in lifestyle similar to the effects of PC1 and weight, such as increased smoking and exposure to tobacco. Changes in alcohol consumption indicated an increase in overall alcohol consumption, with a decrease in wine in favour of spirits, and alcohol being more often taken outside of meals. Finally, both PC2 and BMI reduced physical activity (e.g. reduced duration of walking for pleasure and increased time spent watching TV).

PC3 (abdominal fat distribution) was only significantly associated with increased alcohol intake frequency (b = 0.049, p = $1.1*10^{-6}$) and increased napping during the day (b = 0.046, p = $3.1*10^{-6}$), both of which were similarly affected by WHR (Figure 6, Supplementary Table 14). In addition to these, WHR was associated with many effects attributable to its correlation with BMI, such as reduced income and education. Overall, the effects of PC3 on lifestyle were somewhat similar to those of PC2 (Pearson r = 0.52, p = $1.1*10^{-4}$) and although other causal effects did not reach Bonferroni-corrected significance, many nominally significant results are worth comparing with those from PC2. Many effects on alcohol-related phenotypes were directionally consistent with those of PC2, though 1.9 to 3.8 times weaker. Similarly, the effects on several SES-related phenotypes, such as income and education, were nominally significant though up to 7.5 times weaker than those of PC2. In contrast, none of the measures of physical activity were even nominally significant, despite being among those most strongly affected by PC2. Among smoking-related phenotypes, only those relating to exposure to smoke were nominally significant.

PC4 (lean mass) was associated with greater income (b = 0.052, p = $7.7*10^{-6}$) and increased physical activity, such as frequency of stair climbing and reduced time spent watching TV (Figure 6, Supplementary Table 14).

## Diet

PC1 and weight were associated with greater reported variation in diet (PC1: b = 0.043, p = $1.1*10^{-7}$;weight: b = 0.064, p = $2.9*10^{-12}$) and increased consumption of healthy foods such as fresh fruit and vegetables (Supplementary Table 15). Consumption of coffee was also increased (PC1: b = 0.076, p = $4.6*10^{-17}$; weight: b = 0.088, p = $2.9*10^{-17}$).

PC2 and BMI were similarly associated with reportedly increased variation in diet, though the estimated effects were stronger (PC2: b = 0.099, p = $9.8*10^{-19}$; BMI: b = 0.12, p = $7.1*10^{-29}$). Healthy food intake such as fresh fruits and vegetables was also increased by BMI, though PC2 only weakly increased vegetable intake (Supplementary Table 15). Other changes in diet reflect increased consumption of cheaper meats, namely pork and poultry, while decreasing intake of grain products (bread and cereal), cheese, and dried fruits.

PCs 3 and 4 were not associated with any changes in diet, but WHR was associated with increased consumption of poultry (b = 0.045, p = $2.6*10^{-5}$) and decreased cheese (b = -0.055, p = $5.1*10^{-6}$), consistent with the effects of BMI.

## Brain

As sex-specific summary statistics were not available for brain anatomy, we used the sex-combined summary statistics for both exposure and outcome.

PC1 and weight were associated with reductions in several global measures of brain anatomy, including white matter surface area (b = -0.1, p < $5*10^{-7}$), and grey matter volume and surface (b < -0.09, p < $5*10^{-8}$, Supplementary Table 16). Neither BMI, WHR nor any of the other top PCs were associated in any differences in brain morphometrics, though standing height was associated with decreased volume of ventricles and cerebro-spinal fluid (CSF) (b < -0.12, p < $2.9*10^{-7}$).

Rather than true causal effects, it is likely that these results are due to the use of total intracranial volume (TIV), which represents a proxy for head circumference and size, as a

covariate in the GWAS[25,26]. For example, although brain volume is positively associated with standing height (linear regression slope = 0.55, $p < 10^{-300}$), the association was negative after correction for TIV (slope = -0.14, $p = 10^{-51}$). While the objective of this correction for TIV is to obtain comparable measures across individuals and be able to estimate atrophy without a baseline measure, we found this procedure to overcorrect and induce a negative association between the adjusted regional brain morphometry and height, which is unlikely to be due to atrophy. This overcorrection of regional brain volumes may introduce an undesirable bias in any downstream analyses by creating an arbitrary link between height and brain volume/atrophy. As such, we have not further interpreted the results from brain IDPs.

## Sex-specific effects

The genetic effects of IVs on BMI, weight, and PCs 1, 2, and 4 were not significantly different between men and women, which allowed us to obtain unbiased causal effect estimates using sex-specific summary statistics for the sex of interest in the outcome but the opposite sex in the exposure. The genetic effects of IVs on PC3 and WHR, however, were stronger in women than in men (Wilcoxon: $p_{PC3} = 1.1*10^{-44}$, $p_{WHR} = 8.9*10^{-19}$) and could not be used to test for sex-specific causal effects. Other methods to test for this were considered, but the low statistical power for men in PC3 and strong heterogeneity in WHR produced no significant results.

The low statistical power for testing for differences between sexes led to few results surviving multiple testing correction (full results are listed in Supplementary Tables 17–24). The effects of PC2 on disease risk and lifestyle tended to be stronger in men (TLS $slope_{disease} = 1.19$, $p = 3.8*10^{-3}$; $slope_{lifestyle} = 1.16$, $p = 2.5*10^{-3}$). The effects of PC2 on CVD in particular were consistently almost twice as strong in men ($b_m > 0.11$, $b_f < 0.062$, $p_{diff} = 6.2*10^{-5}$). BMI showed a trend for greater risk of heart disease in men which was only significant for angina ($b_m = 0.12$, $b_f = 0.052$, $p_{diff} = 1.9*10^{-4}$).

## Bi-directional MR

The stringency of the selection criteria for IVs, namely that they be GWS for the sex used as exposure, resulted in few exposures significantly affecting the body traits or PCs. In addition to testing which environmental factors may affect body shape, we were interested in feedback loops, either positive if the forward and reverse causal effects were of the same sign and negative otherwise. The full results are listed in Supplementary Tables 25–28.

Hip circumference increased the risk of diabetes (b = 0.088, p = $5.5*10^{-11}$), which in turn decreased hip circumference (b = -0.22, p = $9*10^{-6}$) in a negative feedback loop. This negative feedback loop with diabetes was nominally significant for several other traits, such as BMI and weight, but not for any of the PCs. Hypercholesterolemia also had nominally significant negative feedback loops, decreasing traits such as weight and BMI, whereas ischaemic heart disease had a similar feedback loop decreasing PC2 and traits such as body fat percentage but not BMI. Waist circumference showed a significant negative feedback loop, increasing the frequency of alcohol consumption, which in turn reduced waist circumference (effect of waist on alcohol: b = 0.18, p = $8.1*10^{-25}$; reverse: b = -0.3, p = $9*10^{-5}$). Similar feedback loops were present for many traits, including BMI, body fat percentage, and weight, but not PCs.

BMI and WHR showed positive feedback loops with both time spent watching TV (effect of BMI on TV: b = 0.16, p = $1.4*10^{-28}$; reverse: b = 0.41, p = $5.7*10^{-5}$; effect of WHR on TV: b = 0.052, p = $7.8*10^{-6}$; reverse: b = 0.31, p = $1.3*10^{-6}$) and usual walking pace (effect of BMI on walking pace: b = -0.27, p = $2.4*10^{-111}$; reverse: b = -0.82, p = $3.2*10^{-10}$; effect of WHR on walking pace: b = -0.099, p = $1.1*10^{-14}$; reverse: b = -0.51, p = $6.9*10^{-6}$). Hip and waist circumferences showed some similarities with these effects, with hip circumference showing a positive feedback loop with usual walking pace (effect of hips on walking pace: b = -0.16, p = $5.1*10^{-39}$; reverse: b = -0.58, p = $8.6*10^{-7}$), while waist circumference showed one with time spent watching TV (effect of waist on TV: b = 0.15, p = $7.3*10^{-18}$; reverse: b = 0.45, p = $5.9*10^{-}$

[5]). Note that the magnitude of the reverse effects of these positive feedback loops would imply an unrealistically large fraction of the variance in body traits could be explained by the variance in the exposure, e.g. usual walking pace would explain $0.82^2$ = 67% of the variance of BMI. These indicate a violation of MR assumptions, likely due to confounding, and were not considered further.

PC3 increased napping during the day (b = 0.046, p = $3.1*10^{-6}$) but was negatively affected by it (b = -0.14, p = $2.2*10^{-6}$). Interestingly, testosterone significantly decreased PC3 (b = -0.012, p = $4.6*10^{-5}$).

### DXA-based measures

DXA and MRI technologies provide increased accuracy in measurements of body composition and have been suggested to provide a clearer picture of obesity and its consequences on health[27]. We were able to predict many such traits based on the subset of ~5,000 UK Biobank participants with these phenotypes, including both VAT and SAT with $r^2$ above 0.7 (Supplementary Table 2), but none of these predicted phenotypes had stronger effects on health than the traits included here (see Supplementary Table 29).

## Discussion

By combining multiple traits through PCA, we found that more than 99% of genetically-determined variation in body shape and size (as defined by the 14 selected traits) can be summarized using four independent PCs affecting (1) body size, (2) adiposity, (3) predisposition to abdominal fat deposition, and (4) lean mass, respectively. PCs 1 and 2 were remarkably similar to weight and BMI, respectively, and embody the hallmark of obesity: the excessive accumulation of body mass. Their enrichment for genes expressed in the brain and involved in neuronal signalling is consistent with previous findings[24] suggesting that behavioural changes

are likely one of the major factors underpinning heritable susceptibility to obesity (reviewed in 28). Considering the disproportionate increase in adiposity characterizing PC2, it is unsurprising that it displayed the most detrimental and numerous consequences on health. Shared effects between PCs 1 and 2 highlight diseases whose aetiology involves elements common to both, such as metabolic overexertion in the case of diabetes[29] or the physical burden of a larger body in the case of arthrosis[30]. Even among these, differences in the magnitude of the effect provide indications of additional mechanisms specific to one, such as lipotoxicity and adipocyte inflammation which contribute to the stronger effects observed for PC2[8]. The increased risk of high cholesterol and heart disease for PC2, but not PC1, is consistent with the predominant role of adipose tissue-related dyslipidaemia[8]. Interestingly, the risk of prolapsed disc was increased by PC1 but not PC2, even though high BMI is considered to be a risk factor[31]. The underlying aetiology has been postulated to involve either mechanical overstraining, obesity-associated dysregulation of the metabolic and immune system, or both[32], however the absence of any effect from PC2 (or PC3) in our results supports the role of mechanical stress over any form of lipotoxicity.

Many changes in lifestyle were common between PC1 and PC2, most of which were stronger for PC2 and while the reduced physical activity is expected[33], the link between obesity and smoking is somewhat more complicated. Observational associations between body mass (generally BMI) and smoking have generally shown a U-shaped relationship between them, with current smokers having a lower BMI on average than former or never smokers[34,35], which is thought to be due to nicotine acting as an appetite suppressant[36]. The increased smoking we found for both PC1 and PC2 likely reflects the use of smoking as a strategy for weight loss and is consistent with observational studies showing a positive association in current smokers between the number of cigarettes smoked and the risk of obesity[37].

The intricate relationship between obesity and alcohol consumption has likewise been difficult to characterize, with many studies having found contradictory results due to discrepancies in the

population characteristics, environmental factors, or measures used to quantify alcohol consumption (reviewed in 38). Most of these studies consider obesity as a consequence of alcohol consumption and have in particular suggested beer as a risk factor for obesity and abdominal adiposity[39]. That we found no effect of obesity on beer consumption is consistent with the postulated directionality of the causal relationship between these phenotypes. Our results do, however, suggest a distinct effect of obesity (both PC1 and PC2) increasing the consumption of spirits. The lack of robust genetic instruments to explore the distinct effect of different alcoholic beverages render MR analysis suboptimal to resolve the reverse causations.

Some consequences of PCs 1 and 2 were not shared, but were rather strongly affected by only one. The effects specific to PC2 suggest a strong effect on lifestyle acting through SES, including increased TDI, greater likelihood of a job including physical work, and lower education and income, similar to what has been reported for BMI[40]. The decreased consumption of wine and alcohol taken with meals is also consistent with lower SES[41]. These results are consistent with the well-known observational association between obesity and low SES[42], however recent results suggest that this is due to residual population stratification and non-genetic familial effects[43,44].

Changes in self-reported diet represent a combination of effects which may make them difficult to interpret. The increased coffee consumption associated with PC1 and PC2 is consistent with previous studies showing coffee consumption to be associated with both smoking and alcohol consumption, though the causality remains unclear[45]. Increased dietary variety and salt added to food may reflect a greater desire for palatable foods, possibly due to altered or reduced activation of the reward system, which has been shown to occur in obese individuals (reviewed in 46). The healthy aspects of these dietary shifts, e.g. greater consumption of fruits and vegetables, could possibly represent attempts to eat healthier however this is likely to be highly confounded by biased reporting[47].

PC3, i.e. predisposition to abdominal fat deposition, was of particular interest as a hypothesis-free emergent component affecting body shape while remaining independent of its size or composition. This is in contrast to WHR which is highly correlated with BMI and body fat percentage, particularly in men[48]. The increased waist circumference at the expense of that of the hips suggests a change in body fat distribution, with a shift from subcutaneous (contributing to both hips and waist) to visceral adipose tissue (contributing to waist alone). This is supported by the enrichment for terms related to energy homeostasis and adipose tissue function, which have previously been reported for WHR adjusted for BMI[49], and the impacts on health which appear specific to lipotoxicity and are similar to what has been found for genetic variants affecting subcutaneous-to-visceral adipose tissue ratio[12,13]. The implication of genes expressed in adipose tissues, particularly subcutaneous, is in line with the hypothesis that adipose tissue function, in particular its expandability, may be a critical factor in determining the distribution and impact of excess adiposity[7] and its study may provide pharmaceutical avenues which may reduce health risks associated with obesity. The enrichment of both PCs 3 and 4 (as well as WHR) for genes expressed in several tissues of the digestive tract is not entirely surprising[50], however their strong enrichment for all and most female-specific tissues tested, respectively, was rather unexpected. It is possible that these tissues, and the genes expressed therein or associated sexual hormones, contribute to this phenotype, which could explain the increased variance of PC3 (and more generally WHR) observed in women compared to men. We found testosterone to decrease PC3, which suggests that the strong sexual dimorphism may result from a combination of positive effects from female-specific tissues and inhibitory effects from male-specific ones. The absence of enrichment for male-specific tissues may be due to a small number of genes being involved or the absence of sexual chromosomes in this analysis. Additional studies will be required to determine how these tissues are involved in the regulation of body fat distribution.

The impact of PC3 on lifestyle was considerably weaker than that of PCs affecting body mass accumulation. Although its effects overall are similar to those of PC2, their differences may provide insight into specific mechanisms involved. For example, the absence of any effect of PC3 on physical activity is consistent with the decrease caused by PC2 being driven by the physical burden of excess body mass. The lack of change in smoking habits supports the hypothesis of the increased tobacco smoking observed for PC2 being used as a means to lose weight[37]. In contrast, the changes in alcohol consumption and SES are directionally consistent with those observed for PC2, suggesting these may be affected by similar causal pathways or subject to the same biases from population stratification or non-genetic familial effects[43,44].

Our method enabled the linear combination of traits at the summary statistics-level, mimicking a GWAS performed on a scaled composite trait and providing effect estimates and standard errors on a standardized scale, circumventing the need for individual-level data. Although this approach does require the correlation matrix of the phenotypes, it may be provided from an external cohort of similar distribution or approximated from the summary statistics via cross-trait LD score regression intercept. The combined summary statistics can then be used for any downstream methods, including two sample MR as either exposure or outcome.

While the effects of PC1 (body size) and PC2 (adiposity) were highly similar to those of weight and BMI, respectively, the PCs present the advantage of their genetic contributions being independent (i.e. the genetically predicted traits are uncorrelated) which is not the case for the respective single traits. As a consequence, although the effects of weight and BMI on health were highly correlated, those of PCs 1 and 2 were much less so. The remaining correlation is to be expected, as the excess accumulation of body mass overall, consisting of both fat and lean mass, is likely to cause many of the same effects as a more specific accumulation of body fat, through the shared components of increased adipose mass or physical burden. Furthermore, while the information from multiple body measures is partially

redundant, making it difficult to quantify their individual contributions, high values for several body PCs will cause cumulative consequences on health which may be considered additively. The components produced by this hypothesis-free approach may be more specific, with underlying genetic mechanisms that are more homogeneous than those of single traits, as illustrated by PC3 (predisposition to abdominal fat deposition) which showed the strongest enrichment for the widest array of biological pathways.

The robustness of the PCs to changes in trait selection or the use of men- *vs* women-specific data supports the hypothesis that these represent true biological mechanisms underlying the correlation across these anthropometric traits. These PCs had some similarities to the average PCs (avPCs) obtained by Ried et al.[11] by meta-analysing PCs from individual-level phenotypic data for BMI, height, weight, WHR, waist and hip circumferences. In particular, both our PC1 and their avPC1 showed a concordant change in all included traits, though height contributed much more strongly to PC1 in our results. The second components both opposed height to BMI and WHR, though in our results the loading for WHR was much weaker. The loadings for avPC3 were dominated by WHR, much like those of PC3, but they also included strong contributions from height and BMI which were much weaker in our results (but directionally consistent). Loadings for the fourth component diverged somewhat between the two approaches, but the increased weight and BMI despite decreased waist and hip circumferences in avPC4 suggest increased body density, which may indicate an increased proportion of lean mass similar to what we observed in PC4. While both methods produce somewhat similar results, the main dissimilarities most likely arise from the fact that we used many more anthropometric traits as well as their inclusion of environmental correlation (i.e. phenotypic correlation caused by shared environmental determinants[51]) in the construction of phenotypic avPCs, which is largely excluded in our approach, with the exception of potential gene-environment correlation. This focus on genetically determined correlation makes our approach better suited to the discovery of biological mechanisms governing body shape, at the cost of discarding behavioural and

environmental factors. While the genetic basis of the composite traits are bound to be orthogonal, their environmental contribution is still somewhat correlated, leading to moderately correlated causal effects (see Supplementary Table 11), which are still much less intertwined than those of individual traits.

The traits used here and currently available in very large sample sizes, namely standard anthropometric traits and bioimpedance-derived estimates, were insufficient to reveal more detailed subtypes of adiposity distribution (e.g. trunk vs. extremities, arms vs legs, etc.) despite including 14 partially independent traits. Although more sophisticated measures of obesity and body shape, such as DXA- and MRI-derived phenotypes, may provide insight into the physiological changes underlying disease aetiology, our results suggest that the increased granularity of observation in many of these measures, such as VAT and SAT, may be insufficient to improve our ability to predict disease risk.

The systematic application of MR over a broad range of phenotypes carries the risk of violating its assumptions. We were able to mitigate the risk of some of these violations through such procedures as filtering out IVs likely affecting the outcome directly (as determined by a larger effect in the outcome than the exposure) or those likely acting through a different pathway (detected by heterogeneity testing). The meta-analysis of cross-sex MR provided a situation similar to a two-sample setting, removing the inflated effect size estimates and false positive rates which would result from a traditional one-sample approach while still making full use of publicly-available summary statistics from a single cohort.

Nevertheless, other sources of bias may remain and affect the MR causal effect estimates. GWAS effect estimates themselves have been shown to be biased due to population effects, such as parental effects, population stratification, and assortative mating[52]. Although such biases in the exposure would not violate the assumptions of MR, their presence in the outcome and any non-genetic effects shared between exposure and outcome may affect MR causal effect estimates[43,44].

In summary, we have applied principal component analysis to summary statistics from individual traits to extract orthogonal aspects (components) of genetics affecting body shape and have developed a composite Mendelian Randomization framework where causal effects of arbitrary linear combinations of exposures on outcomes can be tested using summary statistics alone. The effects of the proposed components of body shape (body size, adiposity, abdominal fat distribution, and lean mass) on hundreds of health-related outcomes and lifestyle factors were assessed, compared to the effects of the individual traits, and can be visualised through the shiny app which can be downloaded by following the instructions at http://wp.unil.ch/sgg/pca-mr/. The genetic basis for the abdominal fat distribution component, in particular, revealed enrichment for a larger variety of tissues, pathways, and biological mechanisms than shown by any individual trait. While these carefully dissected mechanisms have both shared and distinct health consequences, they do not act in isolation and future work is needed to elucidate their intricate interactions. Finally, these findings open new avenues to identify personalised obesity subtypes of individuals and highlight their health consequences.

# Methods

## Data and phenotype selection

We primarily used GWAS summary statistics data derived from the UK Biobank[16], a cohort of approximately 500’000 participants aged 37–73 (median 58). Phenome-wide GWAS in UK Biobank data were performed and the summary statistics made available by the Neale Lab (http://www.nealelab.is/uk-biobank) for 3 different sex groups: men, women, and both sexes combined. This includes effect estimates for 13.7 million SNPs which were tested for association with 4203 unique phenotypes across 361’194 unrelated, white British individuals (167’020 men, 194’174 women). All were adjusted for age, age$^2$, sex, age*sex, age$^2$*sex, and

the top 20 genetic PCs to correct for population stratification. We excluded SNPs from the HLA region (chr6: 28,477,797 - 33,448,354, www.ncbi.nlm.nih.gov/grc/human/regions/MHC?asm=GRCh37). For continuous phenotypes, we used effect estimates for the inverse rank-normalized trait. For binary traits, we divided the effect estimates and standard errors by the square root of the variance of the trait (that of the analysed sample where provided, otherwise across a similar subset of the UK Biobank). As such, all effects are expressed on the standard deviation (SD) scale and comparable with continuous traits. In addition, we used GWAS summary statistics for brain imaging-derived phenotypes (IDPs) obtained from[25], also calculated in the UK Biobank. Summary statistics for WHR were obtained from a meta-analysis[17] of the GIANT consortium and UK Biobank. In total, 1,458 phenotypes had at least one genome-wide significant (GWS) SNP ($p < 5*10^{-8}$) were divided into 6 mutually exclusive categories: body measures (14 phenotypes), continuous measures of health (37 phenotypes), brain IDPs (1206 phenotypes), dietary habits (19 phenotypes), diseases (125 phenotypes), and lifestyle factors (57 phenotypes), which are briefly described below. The full list of selected phenotypes can be found in Supplementary table 1.

Body measures included BMI, height, weight, hip and waist circumference and WHR, as well as bioimpedance-derived fat and lean mass estimates in arms, legs, trunk, and overall body fat percentage. For arms and legs, summary statistics were available for left and right sides. As these were almost identical, the statistics for the left side alone were used. Basal metabolic rate was also included in body measurements as it is derived from bioimpedance measures, resulting in high correlation with the body composition estimates.

Continuous health outcomes included the biomarker panel of the UK Biobank, including 34 biomarkers measured in either blood or urine, as well as systolic and diastolic blood pressure (BP), heart rate at rest and during effort, and forced vital capacity (FVC).

For brain IDPs, we included 3,144 IDPs for which summary statistics were available[25] for a total of 3'144 IDPs, 1’206 of which had at least one genome-wide significant SNP. These

include volumetric, area and thickness measurements of brain regions as well as functional MRI.

Dietary habits were obtained from a food frequency questionnaire (FFQ). UK Biobank also includes more specific questions such as 24-hour recall (food consumed in the last day) which is more reliable but less representative, as well as specific questions such as the type of bread or milk typically consumed, however these were not included in the present analysis.

Disease summary statistics in the UK Biobank were available for self-reported disease status, ICD-10-classified hospital diagnoses, and diseases curated by the Neale Lab in collaboration with the FinnGen consortium (www.finngen.fi). We included data from both self-reported answers and the FinnGen curated diseases, excluding the raw ICD10 diagnoses which were considered less informative. We included any diseases which had a prevalence of at least 1% in the analysed sample.

Lifestyle included both environmental factors and lifestyle choices, mainly relating to physical activity, alcohol consumption, smoking, sleep, work, and socio-economic status.

We compiled a list of SNPs that were common to all our sources of summary statistics. This resulted in 9,559,133 SNPs. SNPs were pruned using the TwoSampleMR R package[53] to obtain independent MR instruments. SNPs were considered independent if separated by more than 10Mb or the linkage disequilibrium was $r^2 < 0.01$.

## High-accuracy body composition measurements

In addition to bioimpedance measurements, the UK Biobank provides other body composition phenotypes derived from more accurate methods, namely DXA and MRI. Unfortunately, the sample sizes for these phenotypes were too low (~5’000 individuals) for their inclusion as body phenotypes in the PCA. We did, however, investigate whether approximating these traits through linear combination of other available traits (with regression weights calculated in the UK Biobank) could provide a hypothesis-driven alternative to the hypothesis-free PCA approach.

We were able to estimate 57 body composition measurements using the same 14 anthropometric and bioimpedance-based traits with varying accuracy (see Supplementary Table 2). 18 out of 57 had an $r^2$ above 80%, including abdominal SAT, and another 18 had $r^2$ above 70%, including VAT. Others, such as bone mass and liver fat percentage could not be accurately approximated using the included traits.

## Principal component analysis

Principal component analysis (PCA) was performed on a matrix of effect estimates of independent SNPs on the 14 body traits described above. We selected all SNPs with a genome-wide significant (GWS) effect ($p < 5*10^{-8}$) on at least one of the body traits and pruned them using the same procedure as for single traits (distance > 10Mb or $r^2 < 0.01$). SNPs were prioritized according to the highest rank within any significantly associated trait, i.e. for each trait, all SNPs significantly associated with it were ranked by p-value; then each SNP was attributed a priority based on the highest rank obtained with any significantly associated trait. This was done to avoid the well-powered traits (e.g. height) overshadowing other traits and driving the SNP selection. Any missing effect estimates in the resulting matrix were set to 0. Data was neither centred nor scaled prior to the PCA, as the effect estimates were standardized and should therefore have zero mean and their variance for a given trait is informative (distantly related to trait heritability). For reproducibility and ease of interpretation and comparison, the loadings were lined up so as to have a positive (even if non-significant) contribution for BMI.

To maintain comparable effects between PCs and traits we scaled the PC loadings such that the resulting βs represent SNP effects on composite traits scaled to have unit variance:

$$v_i = \frac{w_i}{\sqrt{w_i^T K w_i}},$$

where $w_i$ and $v_i$ are the unadjusted and adjusted (trait) loading vectors for PC i, respectively. K is the pairwise phenotypic correlation matrix of body trait phenotypes, which was calculated

on a subset of the UK Biobank similar to that used for the summary statistics (i.e. unrelated white British individuals) and the phenotypes were corrected for the same covariates as used by the Neale lab prior to calculating the correlation. The effect estimates were then calculated using these adjusted loadings, i.e.

$$\beta_i = \hat{B} * v_i,$$

where $\hat{B}$ is the matrix of genetic effects on the 14 anthropometric traits. The corresponding standard errors were calculated following the formula for a weighted sum of random variables:

$$\hat{\sigma}_{i,j}^2 = w_i^T \cdot \Sigma_j \cdot K \cdot \Sigma_j \cdot w_i,$$

where $\hat{\sigma}_{i,j}$ is the standard error for the association of SNP j with PC i and $\Sigma_j$ is a diagonal matrix with the standard error of the association of SNP j with each trait. Since we use only UK Biobank summary statistics, the correlation between effect estimates simplifies to the phenotypic correlation between the traits. The advantage of this approach is that we do not need to calculate the composite trait and run a GWAS, but can directly compute the association summary statistics.

## Tissue specificity and pathway enrichment

We tested PC- and trait-associated SNPs for enrichment of tissue-specific genes using the MAGMA tool for gene set analysis[18] through the FUMA v 1.3.5e interface[19] using the default parameters, with a Bonferroni-adjusted p-value threshold. We used gene expression data in 54 tissues from GTEx v8[20] as well as brain development and age data from BrainSpan[21].

We used the molecular pathway gene sets defined by DEPICT[22] and tested for enrichment using PASCAL[23].

## Mendelian randomization

We used inverse-variance weighted (IVW) Mendelian randomization (MR) to estimate causal effects of body traits and PCs on all non-body traits, as well as the reverse. MR mimics a randomized controlled trial (RCT) where the treatment corresponds to the random allocation of an exposure-associated allele, called an instrumental variable (IV)[54]. MR relies on three key assumptions to infer causality: 1, the IV is associated with a change in the exposure; 2, the IV is independent of the outcome, except through its association with the exposure; 3, the IV is independent of any confounders of the exposure-outcome association. If these assumptions are verified, MR provides an unbiased estimate of the causal effect of the exposure on the outcome and can be done using summary statistics data alone. We used IVW MR as default method for all our analyses, but we compared IVW causal effect estimates to those obtained from weighted median-based MR to ensure robustness.

## Cross-sex Mendelian randomization

In our case, the use of summary data from the UK Biobank for both the exposure and outcome effect sizes (i.e. full sample overlap) would lead to a bias in MR causal effect estimate in the direction of the observed correlation of the phenotypes[55]. To circumvent this, we used the existing summary statistics for two non-overlapping samples from the Neale Lab, those for men and women separately. Each sex was used as exposure on the other as outcome and then both causal effect estimates were meta-analysed (using inverse variance weighting). This removed the correlation between the error terms of the effect estimates of IVs on exposure and outcome, significantly reducing the bias from sample overlap, while minimizing loss of power. This will lead to a slight bias away from zero even when there is no true difference in the genetic effects on the exposure in men and women since:

$$\left|\alpha * \frac{\beta_m/\beta_f + \beta_f/\beta_m}{2}\right| \geq |\alpha|,$$

where $\alpha$ is the common causal effect (for men and women), $\beta_m$ and $\beta_f$ are the coefficients of association for a given IV with the exposure for men and women, respectively. This bias will increase if there is a difference between sexes in the strength of association with the exposure, but its magnitude remains small. For example, if the SNP effects on the exposure were consistently 1.37 times stronger in one sex, the relative theoretical bias would only be 5%. In practice, however, the IVs were filtered for genome-wide significance in each sex prior to being used as exposure, resulting in fewer IVs being selected in the sex with weaker effects (on the exposure). This reduced power and increased variance in the overestimated causal effect, which was correspondingly down-weighted by the IVW meta-analysis. For example, we found PC3 to have a strong sex-specificity, with effects on exposure tending to be ~2.1 times stronger in women, which would theoretically lead to a 28% bias away from the null. However, this yielded 285 GWS SNPs selected as IVs in women but only 47 in men. This increased the variance in the male exposure - female outcome causal effect estimate by a median of 7.8-fold, resulting in a corresponding down-weighting of the overestimated causal effect. In this example, we expect a meta-analysed estimate which is biased towards the null by ~34% (since the IVW causal effect estimate is expected to be ((7.8/8.8)*(1/2.1) + (1/8.8)*2.1)*$\alpha$=0.66*$\alpha$). Importantly, since the bias is multiplicative, our approach has no bias in the absence of causal effect, indicating it will not affect the type I error rate.

Despite relying on sex-specific effect estimates, we selected IVs based on their sex-combined exposure association. This not only reduces winner's curse, but also gives us a common set of SNPs from which to draw IVs, making the enrichment analyses more meaningful and ensuring that the results are comparable across sexes and the causal effects to be meta-

analysed are equivalent. These IVs were filtered for genome-wide significance in the sex-specific summary statistics prior to MR analysis to avoid weak instrument bias.

For each sex, the GWS SNPs associated with the exposure formed the initial set of IVs. Those with significantly larger effects on the outcome than on the exposure were removed, as these would indicate a violation of MR assumptions (likely reverse causality and/or confounding). The effect sizes being on a standardized scale, they were compared directly using a one-sided t-test and removed if the effects in the outcome were significantly greater ($p < 0.05$). To avoid unreliable causal effect estimates, MR was only performed if at least 10 IVs remained. This was done using the *TwoSampleMR* R package[53].

The MR causal effect estimates from individual IVs were tested for heterogeneity using Cochran's Q test:

$$Q_i = \frac{(\beta_{i_{out}} - \beta_{MR} * \beta_{i_{exp}})^2}{\sigma^2_{i_{out}} + \beta^2_{i_{exp}} * \sigma^2_{MR} + \beta^2_{MR} * \sigma^2_{i_{exp}} + \sigma^2_{MR} * \sigma^2_{i_{exp}}},$$

where $\beta_{iexp}$ and $\beta_{iout}$ are the coefficients of association of SNP i with the exposure and outcome, respectively, with $\sigma_{iexp}$ and $\sigma_{iout}$ the corresponding standard errors, and $\beta_{MR}$ and $\sigma_{MR}$ are the MR estimate and standard error of the causal effect of the exposure on the outcome. The test statistic $Q_i$ follows a $\chi^2$ distribution with 1 degree of freedom. If any of the IVs used had an associated $p < 10^{-4}$, the most heterogeneous one (with the lowest p-value) was removed. If at least 5 IVs remained, the MR was then repeated with the remaining IVs.

Due to the standardized scales of IV effect estimates, the resulting causal effects are on a scale representing the SD change in the outcome for a change of 1 SD in the exposure.

To account for multiple testing, we adjusted the p-value threshold with Bonferroni correction for the number of tests within the exposure-outcome category pair. For example, the p-value threshold for the effect of BMI (body phenotype) on T2D (disease) is 0.05 / (number of body phenotypes * number of diseases).

## Sex-specific Mendelian randomization

The simplest method to test for sex-specific effects would be to use sex-specific summary statistics for the sex of interest for both exposure and outcome. This would bias results away from the null due to correlated errors in the exposure and outcome but would affect men and women similarly, assuming the environmental confounding is consistent between sexes. While this would lead to overestimated causal effects, it would not inflate the false positive rate of detected differences between sexes.

In many cases, we were instead able to obtain unbiased causal effect estimates using the exposure summary statistics from the opposite sex. This relied on the strength of the association between the IVs and the exposure to be identical (or at least not systematically different) between sexes. We tested this using both paired Wilcoxon signed-rank test on the absolute genetic effects of the IVs and total least squares (TLS) regression. Exposures with non-significant results for both tests were considered identical in both sexes for this purpose and the summary statistics for the opposite sex were used for the exposure.

## Comparison of causal effects

To test the significance of a difference in effects of two exposures on a given outcome, we used a two-sided Z-test[56]. We accounted for multiple testing using Bonferroni correction, adjusting for the total number of tests, i.e. the number of significant effects of either exposure on the category outcomes. For example, to test whether the effects of BMI on T2D were different from those of WHR, the significance threshold would be 0.05 / total number of diseases significantly affected by either BMI or WHR.

In some cases, it was useful to compare the causal effects of two exposures on all outcomes of a category (e.g. the effects of weight on disease risk compared to those of PC1) or the same exposure in different experimental settings (comparison of methods or sex-stratified analyses).

In these cases, we obtained the slope estimate using TLS regression with no intercept, which considers error in both axes rather than ordinary least squares (OLS) which minimizes only the vertical offset. The standard error on the angle of the regression line (rather than the slope, which is not symmetrical and dependent on the phenotype placed on the y-axis) was computed using a jackknife procedure, which was then used to compare the obtained estimate with the null hypothesis that the true causal effects were identical (i.e. an angle of 45° or a slope of 1). The TLS procedure was performed using the *deming* R package[57].

## Acknowledgements

This research has been conducted using the UK Biobank resource (#16389), which has been approved by the National Research Ethics Service Committee. The computations have been carried out on the HPC server of the Lausanne University Hospital. Z.K. was funded by the Swiss National Science Foundation (31003A-143914 and 310030-189147). B.D. is supported by the Swiss National Science Foundation (NCCR Synapsy, project grant Nr. 32003B_135679, 32003B_159780, 324730_192755 and CRSK-3_190185) and the Leenaards Foundation. LREN is very grateful to the Roger De Spoelberch and Partridge Foundations for their generous financial support. T.O.K. was funded by the Novo Nordisk Foundation (NNF17OC0026848, NNF18CC0034900).

## Author contributions

A.S. and J.S. pre-processed the data and performed the initial analyses. N.M. assisted with initial data pre-processing. B.D. contributed to the initial design and the analysis and interpretation of brain imaging results. J.S. developed the methods and performed the remaining analyses. Z.K. supervised the project. J.S. wrote the initial manuscript. All authors provided critical feedback, helped interpret the findings and improve the manuscript.

## References


1. Boles, A., Kandimalla, R. & Reddy, P. H. Dynamics of diabetes and obesity: Epidemiological perspective. *Biochim. Biophys. Acta Mol. Basis Dis.* **1863**, 1026–1036 (2017).
2. Ortega, F. B., Lavie, C. J. & Blair, S. N. Obesity and Cardiovascular Disease. *Circ. Res.* **118**, 1752–1770 (2016).
3. Pischon, T. *et al.* General and abdominal adiposity and risk of death in Europe. *N. Engl. J. Med.* **359**, 2105–2120 (2008).
4. Kaess, B. M. *et al.* The ratio of visceral to subcutaneous fat, a metric of body fat distribution, is a unique correlate of cardiometabolic risk. *Diabetologia* **55**, 2622–2630 (2012).
5. Rosenquist, K. J. *et al.* Visceral and subcutaneous fat quality and cardiometabolic risk. *JACC Cardiovasc. Imaging* **6**, 762–771 (2013).
6. Abraham, T. M., Pedley, A., Massaro, J. M., Hoffmann, U. & Fox, C. S. Association between visceral and subcutaneous adipose depots and incident cardiovascular disease risk factors. *Circulation* **132**, 1639–1647 (2015).
7. Virtue, S. & Vidal-Puig, A. Adipose tissue expandability, lipotoxicity and the Metabolic Syndrome--an allostatic perspective. *Biochim. Biophys. Acta* **1801**, 338–349 (2010).
8. Heymsfield, S. B. & Wadden, T. A. Mechanisms, Pathophysiology, and Management of Obesity. *The New England journal of medicine* vol. 376 1492 (2017).
9. Zhang, M., Hu, T., Zhang, S. & Zhou, L. Associations of Different Adipose Tissue Depots with Insulin Resistance: A Systematic Review and Meta-analysis of Observational Studies. *Sci. Rep.* **5**, 18495 (2015).
10. Porter, S. A. *et al.* Abdominal subcutaneous adipose tissue: a protective fat depot?

*Diabetes Care* **32**, 1068–1075 (2009).

11. Ried, J. S. *et al.* A principal component meta-analysis on multiple anthropometric traits identifies novel loci for body shape. *Nat. Commun.* **7**, 13357 (2016).
12. Yaghootkar, H. *et al.* Genetic evidence for a normal-weight 'metabolically obese' phenotype linking insulin resistance, hypertension, coronary artery disease, and type 2 diabetes. *Diabetes* **63**, 4369–4377 (2014).
13. Yaghootkar, H. *et al.* Genetic Evidence for a Link Between Favorable Adiposity and Lower Risk of Type 2 Diabetes, Hypertension, and Heart Disease. *Diabetes* **65**, 2448–2460 (2016).
14. Lotta, L. A. *et al.* Integrative genomic analysis implicates limited peripheral adipose storage capacity in the pathogenesis of human insulin resistance. *Nat. Genet.* **49**, 17–26 (2017).
15. Ji, Y. *et al.* Genome-Wide and Abdominal MRI Data Provide Evidence That a Genetically Determined Favorable Adiposity Phenotype Is Characterized by Lower Ectopic Liver Fat and Lower Risk of Type 2 Diabetes, Heart Disease, and Hypertension. *Diabetes* **68**, 207–219 (2019).
16. Sudlow, C. *et al.* UK biobank: an open access resource for identifying the causes of a wide range of complex diseases of middle and old age. *PLoS Med.* **12**, e1001779 (2015).
17. Pulit, S. L. *et al.* Meta-analysis of genome-wide association studies for body fat distribution in 694,649 individuals of European ancestry. *bioRxiv* 304030 (2018) doi:10.1101/304030.
18. de Leeuw, C. A., Mooij, J. M., Heskes, T. & Posthuma, D. MAGMA: generalized gene-set analysis of GWAS data. *PLoS Comput. Biol.* **11**, e1004219 (2015).
19. Watanabe, K., Taskesen, E., van Bochoven, A. & Posthuma, D. Functional mapping and annotation of genetic associations with FUMA. *Nat. Commun.* **8**, 1826 (2017).
20. Aguet, F. *et al.* The GTEx Consortium atlas of genetic regulatory effects across human tissues. *bioRxiv* 787903 (2019) doi:10.1101/787903.
21. Miller, J. A. *et al.* Transcriptional landscape of the prenatal human brain. *Nature* **508**, 199–

206 (2014).

22. Pers, T. H. *et al.* Biological interpretation of genome-wide association studies using predicted gene functions. *Nature Communications* vol. 6 (2015).
23. Lamparter, D., Marbach, D., Rueedi, R., Kutalik, Z. & Bergmann, S. Fast and Rigorous Computation of Gene and Pathway Scores from SNP-Based Summary Statistics. *PLOS Computational Biology* vol. 12 e1004714 (2016).
24. Locke, A. E. *et al.* Genetic studies of body mass index yield new insights for obesity biology. *Nature* **518**, 197–206 (2015).
25. Elliott, L. T. *et al.* Genome-wide association studies of brain imaging phenotypes in UK Biobank. *Nature* **562**, 210–216 (2018).
26. Smith, S. M. *et al.* Accurate, robust, and automated longitudinal and cross-sectional brain change analysis. *Neuroimage* **17**, 479–489 (2002).
27. Marra, M. *et al.* Assessment of Body Composition in Health and Disease Using Bioelectrical Impedance Analysis (BIA) and Dual Energy X-Ray Absorptiometry (DXA): A Critical Overview. *Contrast Media Mol. Imaging* **2019**, 3548284 (2019).
28. van der Klaauw, A. A. & Farooqi, I. S. The hunger genes: pathways to obesity. *Cell* **161**, 119–132 (2015).
29. Halban, P. A. *et al.* β-cell failure in type 2 diabetes: postulated mechanisms and prospects for prevention and treatment. *Diabetes Care* **37**, 1751–1758 (2014).
30. Duclos, M. Osteoarthritis, obesity and type 2 diabetes: The weight of waist circumference. *Ann. Phys. Rehabil. Med.* **59**, 157–160 (2016).
31. Schroeder, G. D., Guyre, C. A. & Vaccaro, A. R. The epidemiology and pathophysiology of lumbar disc herniations. *Semin. Spine Surg.* **28**, 2–7 (2016).
32. Weiler, C. *et al.* Histological analysis of surgical lumbar intervertebral disc tissue provides evidence for an association between disc degeneration and increased body mass index. *BMC Res. Notes* **4**, 497 (2011).

33. Richmond, R. C. *et al.* Assessing causality in the association between child adiposity and physical activity levels: a Mendelian randomization analysis. *PLoS Med.* **11**, e1001618 (2014).

34. Sneve, M. & Jorde, R. Cross-sectional study on the relationship between body mass index and smoking, and longitudinal changes in body mass index in relation to change in smoking status: the Tromso Study. *Scand. J. Public Health* **36**, 397–407 (2008).

35. Mackay, D. F., Gray, L. & Pell, J. P. Impact of smoking and smoking cessation on overweight and obesity: Scotland-wide, cross-sectional study on 40,036 participants. *BMC Public Health* **13**, 348 (2013).

36. Mineur, Y. S. *et al.* Nicotine decreases food intake through activation of POMC neurons. *Science* **332**, 1330–1332 (2011).

37. Dare, S., Mackay, D. F. & Pell, J. P. Relationship between smoking and obesity: a cross-sectional study of 499,504 middle-aged adults in the UK general population. *PLoS One* **10**, e0123579 (2015).

38. Traversy, G. & Chaput, J.-P. Alcohol Consumption and Obesity: An Update. *Curr. Obes. Rep.* **4**, 122–130 (2015).

39. Bendsen, N. T. *et al.* Is beer consumption related to measures of abdominal and general obesity? A systematic review and meta-analysis. *Nutr. Rev.* **71**, 67–87 (2013).

40. Howe, L. D. *et al.* Effects of body mass index on relationship status, social contact and socio-economic position: Mendelian randomization and within-sibling study in UK Biobank. *Int. J. Epidemiol.* (2019) doi:10.1093/ije/dyz240.

41. Oksanen, A. & Kokkonen, H. Consumption of Wine with Meals and Subjective Well-being: A Finnish Population-Based Study. *Alcohol Alcohol* **51**, 716–722 (2016).

42. Wang, Y. & Beydoun, M. A. The Obesity Epidemic in the United States Gender, Age, Socioeconomic, Racial/Ethnic, and Geographic Characteristics: A Systematic Review and Meta-Regression Analysis. *Epidemiologic Reviews* vol. 29 6–28 (2007).

43. Darrous, L., Mounier, N. & Kutalik, Z. Simultaneous estimation of bi-directional causal effects and heritable confounding from GWAS summary statistics. *Genetic and Genomic Medicine* (2020) doi:10.1101/2020.01.27.20018929.

44. Brumpton, B. *et al.* Avoiding dynastic, assortative mating, and population stratification biases in Mendelian randomization through within-family analyses. *Nat. Commun.* **11**, 3519 (2020).

45. Lieberman, H. R., Agarwal, S. & Fulgoni, V. L., 3rd. Daily Patterns of Caffeine Intake and the Association of Intake with Multiple Sociodemographic and Lifestyle Factors in US Adults Based on the NHANES 2007-2012 Surveys. *J. Acad. Nutr. Diet.* **119**, 106–114 (2019).

46. Stice, E., Spoor, S., Ng, J. & Zald, D. H. Relation of obesity to consummatory and anticipatory food reward. *Physiol. Behav.* **97**, 551–560 (2009).

47. Pirastu, N. *et al.* Using genetics to disentangle the complex relationship between food choices and health status. *bioRxiv* 829952 (2019) doi:10.1101/829952.

48. Sulc, J., Winkler, T. W., Heid, I. M. & Kutalik, Z. Heterogeneity in Obesity: Genetic Basis and Metabolic Consequences. *Curr. Diab. Rep.* **20**, 1 (2020).

49. Shungin, D. *et al.* New genetic loci link adipose and insulin biology to body fat distribution. *Nature* **518**, 187–196 (2015).

50. Winkler, T. W. *et al.* A joint view on genetic variants for adiposity differentiates subtypes with distinct metabolic implications. *Nat. Commun.* **9**, 1946 (2018).

51. Searle, S. R. Phenotypic, Genetic and Environmental Correlations. *Biometrics* vol. 17 474 (1961).

52. Young, A. I. *et al.* Mendelian imputation of parental genotypes for genome-wide estimation of direct and indirect genetic effects. *bioRxiv* 2020.07.02.185199 (2020) doi:10.1101/2020.07.02.185199.

53. Hemani, G. *et al.* The MR-Base platform supports systematic causal inference across the human phenome. *eLife* vol. 7 (2018).

54. Burgess, S., Butterworth, A. & Thompson, S. G. Mendelian randomization analysis with multiple genetic variants using summarized data. *Genet. Epidemiol.* **37**, 658–665 (2013).

55. Burgess, S., Davies, N. M. & Thompson, S. G. Bias due to participant overlap in two-sample Mendelian randomization. *Genet. Epidemiol.* **40**, 597–608 (2016).

56. Paternoster, R., Brame, R., Mazerolle, P. & Piquero, A. USING THE CORRECT STATISTICAL TEST FOR THE EQUALITY OF REGRESSION COEFFICIENTS. *Criminology* **36**, 859–866 (1998).

57. Therneau, T. *deming: Deming, Theil-Sen, Passing-Bablock and Total Least Squares Regression, R package version 1.4*. https://CRAN.R-project.org/package=deming (2018).

# Figures

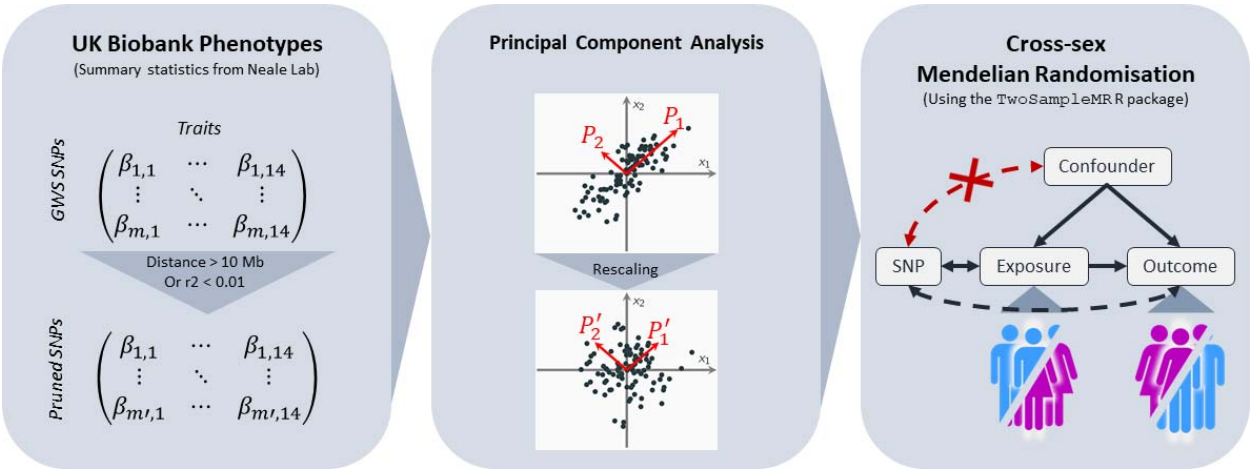


**Figure 1. Overview of the methods.** Summary statistics for anthropometric traits from the UK Biobank were pruned for independence before being subjected to principal component analysis (PCA). The genetic effects on the resulting components were scaled to obtain effect sizes corresponding to a trait with a variance of 1 (standardized). Mendelian randomization was used to determine the impact of these composite traits on lifestyle and health outcomes.

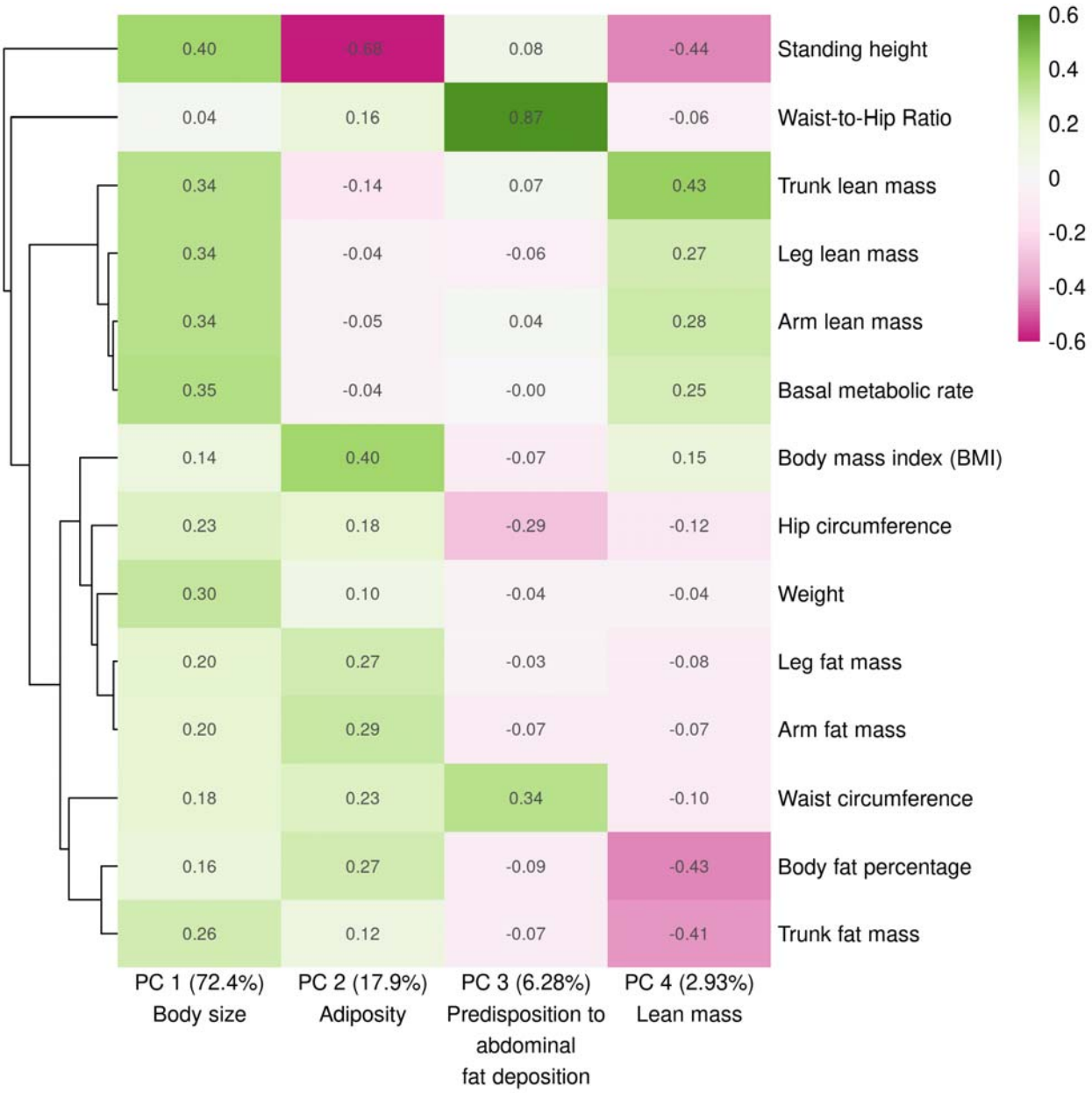


**Figure 2. The contributions of each trait to the first four PCs in women.** The explained variance of each PC is included in parentheses along with the descriptive name used in the main text. The loadings presented here are those typically used in PCA, scaled such that the sum of the squared weights is equal to 1 (as opposed to the scaling used to obtain composite traits with a variance of 1). This provides a consistent scale and makes PCs more easily comparable.

**Figure 3. Body size and accumulation of body fat were mainly enriched for genes expressed in the brain, while the others were enriched for a broader range of tissues.** Enrichment of traits and principal components (PCs) for tissue-specific gene expression (negative log 10 p-values). Genome-wide SNP effect p-values were analysed using MAGMA on GTEx v8 data (54 tissues). Results not significant after Bonferroni correction are masked in white.

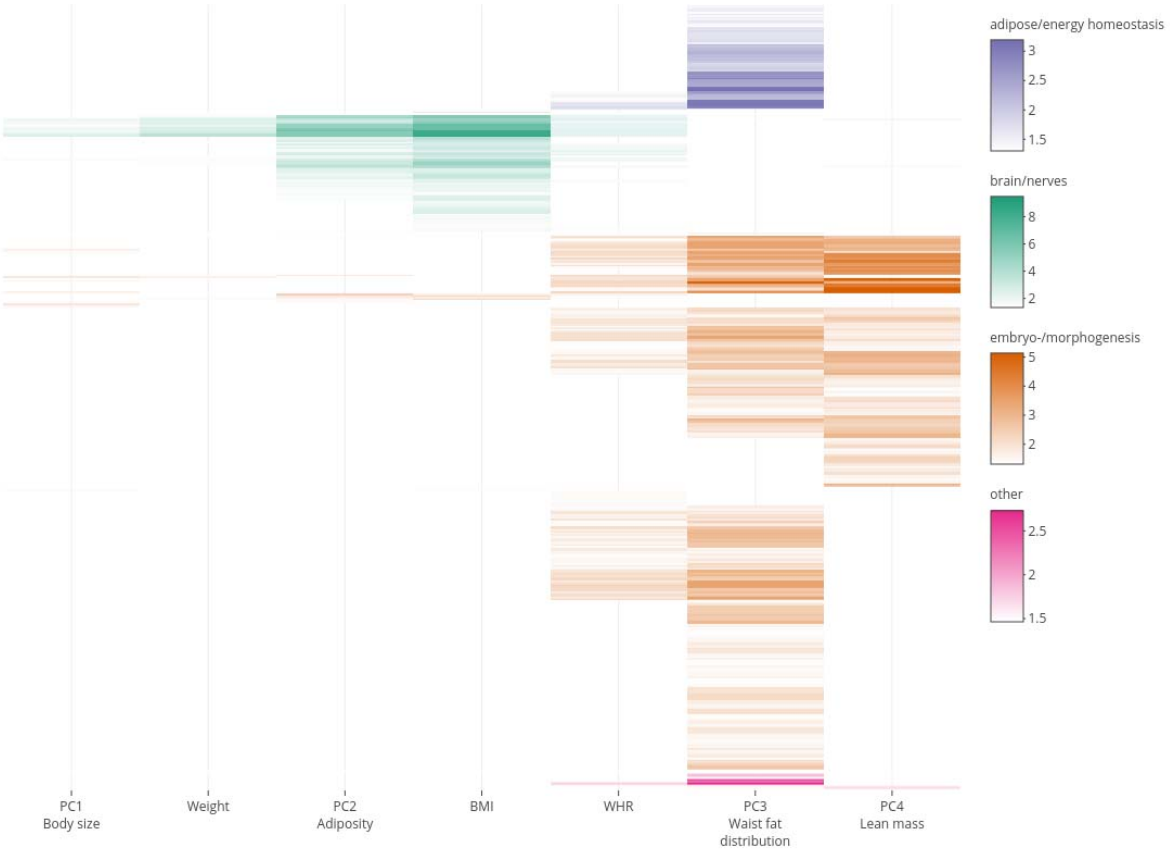


**Figure 4. Pathway enrichment shows a similar distinction between body size/fat mass accumulation *vs* measures of body fat distribution/lean mass.** The enrichment of traits and principal components (PCs) for molecular pathways (negative log 10 p-values). Genome-wide SNP effect p-values were analysed using PASCAL on molecular pathways defined by DEPICT. These were qualitatively split into four categories to aid in interpretation. Pathways which were not significantly enriched in any of the traits/PCs are not shown here.

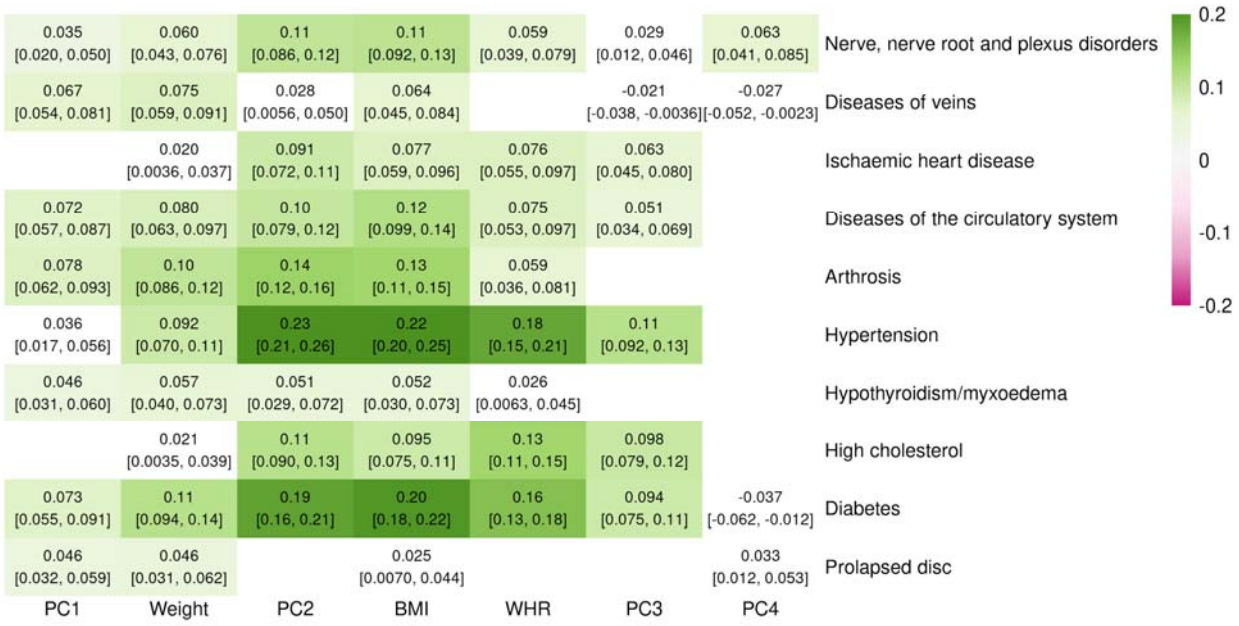


**Figure 5. Single and composite traits increase the risk of multiple diseases.** MR causal effects of traits and principal components (PCs) on a selection of diseases on a standardized scale. The 95% confidence interval of the effect is indicated in brackets. Effects which were not significant at the Bonferroni-corrected threshold ($p < 4.3*10^{-5}$) are coloured in white. The full list of effects can be found in Supplementary table 12.

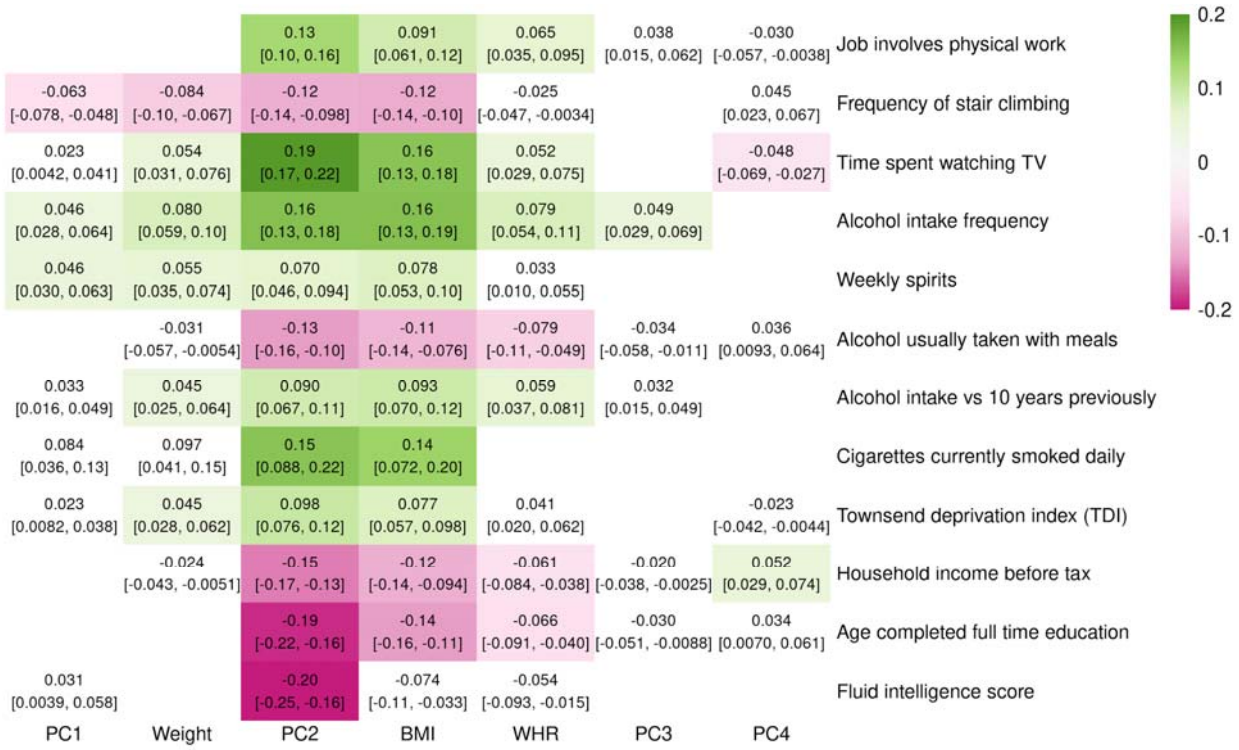


**Figure 6. Single and composite traits affect many aspects of lifestyle.** MR causal effects of traits and principal components (PCs) on a selection of lifestyle factors on a standardized scale. The 95% confidence interval of the effect is indicated in brackets. Effects which were not significant at the Bonferroni-corrected threshold ($p < 7.1*10^{-5}$) are coloured in white. The full list of effects can be found in Supplementary table 13.